ARTICLE

Preparation and Refractive Index of Nano BST Thin Films†

Song-zhan Li[a*], Yan-qin Yang[a], Wen-cong Liu[a], Tian-jin Zhang[b], Ya-jun Qi[b]

a. College of Electronics and Information Engineering, Wuhan University of Science and Engineering, Wuhan 430073, China;
b. Department of Materials Science and Engineering, Hubei University, Wuhan 430062, China

(Dated: Received on August 30, 2007; Accepted on October 10, 2007)

Radio frequency magnetron sputtering technique is used to deposit $Ba_{0.65}Sr_{0.35}TiO_3$ (BST) thin films on fused quartz substrates. In order to prepare the high quality BST thin films, the crystallization and microstructure of the films were characterized by X-ray diffraction, field emission scanning electron microscopy and atom force microstructure. The more intense characteristic diffraction peaks and better crystallization can be observed in BST thin films deposited at 600 °C and subsequently annealed at 700 °C. The refractive index of the films is determined from the measured transmission spectra. The dependences of the refractive index on the deposition parameters of BST thin films are different. The refractive index of the films increases with the substrate temperature. At lower sputtering pressure, the refractive index increases from 1.797 to 2.179 with the pressure increase. However, when the pressure increases up to 3.9 Pa, the refractive index instead reduces to 1.860. The oxygen to argon ratio also plays an important effect on the refractive index of the films. It has been found that the refractive index increases with the ratio of oxygen to argon increasing. The refractive index of BST thin films is strongly dependent on the annealing temperature, which also increases as the annealing temperature ascends. In one word, the refractive index of BST thin films is finally affected by the films microstructure and texture.

Key words: BST thin film, Radio frequency magnetron sputtering, Deposition parameter, Refractive index

I. INTRODUCTION

Ferroelectric thin films are very promising for a wide range of applications such as uncooled infrared detectors and focal plane arrays [1], nonvolatile memories with low switching voltage [2], planar waveguides [3], and electro-optic devices [4]. Among these materials, $Ba_{1-x}Sr_xTiO_3$ thin films have attracted much attention because of its unique combination of large dielectric constant, high refractive index, large electro-optic coefficient and low optical losses [5-9].

There have been several reports on the electrical and ultraviolet-visible optical properties of $Ba_{1-x}Sr_xTiO_3$ thin films [10-14]. Recently, Roy *et al.* reported the optical property in sol-gel derived $Ba_{0.5}Sr_{0.5}TiO_3$ thin films using a 0.1 mol/L precursor solution [15]. Xu *et al.* reported the optical properties of $Ba_{0.7}Sr_{0.3}TiO_3$ thin films [16]. However, no more detailed refractive index of $Ba_{1-x}Sr_xTiO_3$ thin films has been provided. So far, most studies in ferroelectric thin films have focused on the general optical properties, and, to our knowledge, there are no comprehensive reports concentrating on the refractive index of BST thin films varying with the deposition parameters, especially, the sputtering pressure and the ratio of argon to oxygen.

The object of this paper is to prepare the high quality BST thin films and obtain the relationship between the refractive index of BST thin films and the deposition parameters (the substrate temperature, the sputtering pressure, the ratio of argon to oxygen, and the annealing temperature). It is believed that the dependence of the refractive index of BST thin films on the substrate temperature, the sputtering pressure, the ratio of argon to oxygen and the annealing temperature should be important to optimize the design of electro-optic devices, to improve the potential performance to ferroelectric thin film electro-optic devices.

II. EXPERIMENTS

Radio frequency (RF) magnetron sputter techniques have been used to deposit BST thin films on fused quartz. The BST ceramic target was prepared from high purity $BaCO_3$, $SrCO_3$, and TiO_2 powders (purity 99.9%) using standard solid-state process. The powders were mixed in the planetary milling for 4 h using a plastic container with agate balls. Disk-shaped specimens of 70 mm in diameter and 3 mm in the thickness were obtained by the uniaxial pressing at 100 MPa. The disk-like BST is sintered at 1100 °C for 2 h and at 1350 °C for 2 h in order to densify the target.

The substrates were rinsed in acetone, ethanol, distilled water with a supersonic wave apparatus, and dried by nitrogen gas sequentially before being loaded into the growth chamber.

With a fixed target-to-substrate distance, the sput-

†Part of the special issue from "The 6th China International Conference on Nanoscience and Technology, Chengdu (2007)".
*Author to whom correspondence should be addressed. E-mail: liszhan@yahoo.com.cn, Tel: +86-27-87524586, Fax: +86-27-87611511

tering was carried out in an Ar and O_2 (99.99%) atmosphere by supplying 120 W RF power at a frequency of 13.56 MHz. A cryo-pump, coupled with a rotary pump was used to achieve 10 μPa pressure before introducing Ar and O_2. A mixture of oxygen and argon at various mixing ratios ranged from 1:1 to 1:4 with a total flow of 24 sccm. During the sputtering, the substrate temperatures were kept at room temperature (RT), 560, 600, or 650 °C. The temperature was controlled using a feedback-controlled heater. The films were cooled to room temperature before removing them from the deposition system oxygen at a temperature of 650, 700, 750, or 800 °C for 2 h in a tube furnace. Post annealing in oxygen was done to reduce any oxygen deficiency in the films.

Crystalline phases of the BST samples were identified by X-ray diffraction (XRD, Rigakn D/MAX-IIIC). The XRD operating parameters included a Cu Kα of wavelength λ=0.154176 nm, scan speed of 5°/min, and scan range 20°-67°. The surface microstructure and cross-sectional morphology were observed by field emission scanning electron microscopy (FESEM, JOEL JSM 6700F). The surface morphology was examined by atomic force microscopy (AFM; Digital Instruments, Nano-Scope IIIA). The optical transmission spectrum of BST films were measured in the wavelength range of 190-900 nm using a double beam ultraviolet-visible spectrophotometer (Shimadzu UV-1601 UV/VIS). The envelope method was used to calculate the optical constants.

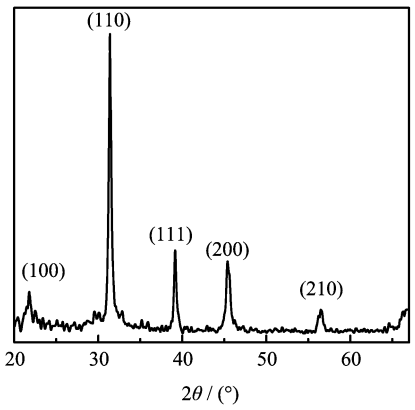

FIG. 1 The XRD patterns of BST thin films deposited at 600 °C and subsequently annealed at 700 °C.

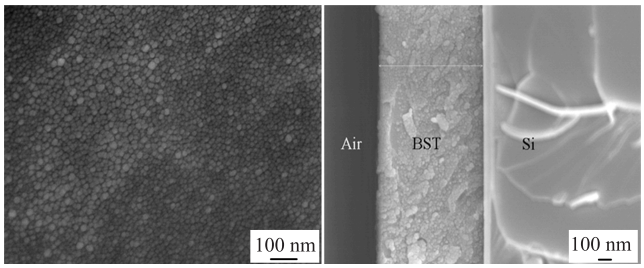

FIG. 2 FESEM photographs of BST thin films deposited at 600 °C and annealed at 700 °C. (a) The surface photograph, (b) The cross-sectional photograph.

III. RESULTS AND DISCUSSION

A. The preparation

The crystallinity of BST films deposited on fused quartz substrate was investigated by XRD spectrum analysis as shown in Fig.1. Figure 1 shows XRD pattern of BST thin films deposited at 600 °C and subsequently annealed at 700 °C. It is evident that the film have a perovskite phase with a pseudocubic structure, and the observed diffraction peaks are (100), (110), (111), (200), and (210) within the 2θ range from 20° to 67°. The results show that the films are polycrystalline without a preferred orientation and contain the perovskite phase only. It is also found that the characteristic XRD peaks is sharp and more intense, indicating an better crystallinity.

Figure 2(a) shows the surface morphology of $Ba_{0.65}Sr_{0.35}TiO_3$ thin film prepared by RF magnetron sputtering. It can be noted from Fig.2(a) that the surface of the BST film annealed at 700 °C is smooth, crack-free and pore-free. The grains of the BST film are evenly distributed and the average grain size is about 50 nm, indicating that $Ba_{0.65}Sr_{0.35}TiO_3$ thin films annealed at 700 °C have a welldefined microstructure.

Figure 2(b) shows a cross-sectional FESEM image of BST film deposited at 600 °C and a pressure of 3.9 Pa, and annealed at 700 °C in a horizontal quartz tube furnace. It can be noted from the picture that the interface between the film and the substrate is sharp and clear, which indicates that the film integrates with the substrate closely and there is no obvious interdiffusion between the film and the substrate.

The AFM morphology also indicates that the film is dense and fine-grained. The average surface roughness of BST thin films is about 10 nm. This fine-grained thin film with a higher packing density and a smaller roughness is more suitable for various optical applications than other ferroelectric thin films [17].

From XRD pattern, and FESEM and AFM images, the above parameters are considered as the optimum for the deposition of $Ba_{0.65}Sr_{0.35}TiO_3$ thin films on fused quartz substrates.

Figure 3 shows the optical transmittance spectra of BST thin films deposited on fused quartz and subsequently annealed at 700 and 800 °C, respectively. The transparency of the films increases sharply at a wavelength of 320 nm, and is above 60% for wavelengths longer than 460 nm. The transparency of the films decreases when postdeposition temperature increases. It is also noted that the absorption edge of the thin film shifts towards longer wavelengths (i.e., lower energy)

DOI:10.1088/1674-0068/20/06/706-710

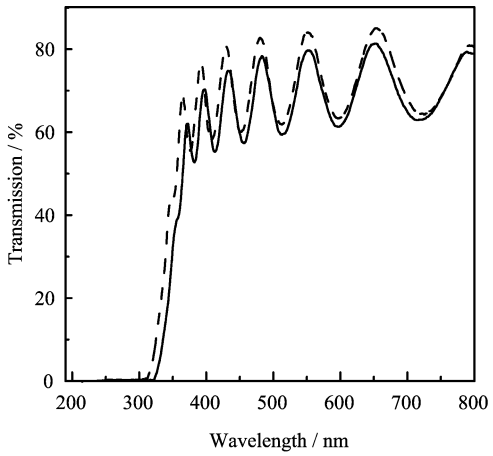

FIG. 3 Optical transmittance spectra of BST thin films deposited on fused quartz substrates: (a) 700 °C (−−); (b) 800 °C (—).

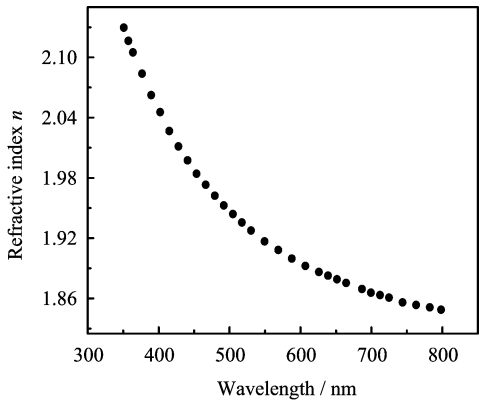

FIG. 4 Refractive index of $Ba_{0.65}Sr_{0.35}TiO_3$ thin films as a function of wavelength.

with increasing postdeposition temperature. This implies a decrease in electron gap energy with increasing crystallite size.

If we assume that the crystallites are spherical, the energy of BST nanocrystallites can be expressed as [18,19]

$$E = E_g + \frac{h^2}{2}\frac{\pi^2}{R^2}\left(\frac{1}{m_e}+\frac{1}{m_h}\right) - 1.78\frac{e^2}{\varepsilon R} - 0.248E^*_{Ry} \quad (1)$$

where E_g is the energy gap, m_e and m_h are the effective masses of the electron and the hole, respectively, R is the radius of the nanocrystallite, ε is the dielectric constant, and E^*_{Ry} is the effective Rydberg energy. The first, second, and third terms on the right side of Eq.(1) correspond to gap energy, size localization energy, and Coulomb interaction energy, respectively, whereas the fourth term arises from the spatial correlation effect, which is usually small. Using Eq.(1), it was shown that the magnitudes of the second and third terms increase with decreasing crystallite size, thereby leading to a change in the eigenenergy state of nanocrystallites and causing a shift of gap energy with decreasing crystallite size. It can be explained by the absorption shifting at different crystallite sizes of the thin films [20].

B. The refractive index

The refractive index n of BST thin films has been determined from the transmittance spectrum following the envelop method of Manifacier *et al.* [21]. The refractive index of BST thin films as a function of wavelength is shown in Fig.4. As can be seen the refractive index in the visible wavelength range is in the reasonable range of 1.85-2.13. The optical function of BST thin films has shown the normal dispersion of the refractive index in the visible range [22].

The refractive index is also a function of substrate temperatures. The observation shows a 10% variation of refractive index for BST thin films deposited over a substrate temperature range of 560 °C to 650 °C without annealing. It can be observed the refractive index increased from 1.778 to 1.961 with substrate temperature rising from 560 °C to 650 °C.

This could be due to the following two reasons. One is the mobility of the particles at different temperatures. At low substrate temperature, the particles with low surface mobility will be located at different positions within the substrate [23]. The low mobility of the particles is not benefit for forming the homogeneous and compact films. The lower packing density, oxygen deficiency and grain boundary result in the lower refractive index of BST thin films.

The other is the minimum total energy of the films. Films grow in such a way that the total energy is minimized [24]. The total energy in any film deposited on a substrate is the sum of three components: the surface energy of the films, the films-substrate interface energy, and the strain energy in the films [25]. At high temperature, the films are inclined to grow in Stranski-Krastanov model [26]. At the earliest stage of film formation, the film surface that grows in Frank-van der Merwe model has higher surface energy. In order to release the energy, the particles try to transfer the exposed crystal plane to the crystal plane with lower energy. The minimum of the total energy of the films is benefit for forming quality films. The increase of the refractive index with substrate temperatures is result form the high quality films formation.

In Fig.5 the refractive index is plotted *vs.* pressure. In the range of the sputtering pressure from 0.37 Pa to 2.5 Pa, the refractive index of as-deposited BST thin films increased from 1.797 to 2.179 with the sputtering pressure increasing. But when the sputtering pressure increases up to 3.9 Pa, the refractive index reduced to 1.860. The behavior of the refractive index results from the different effect of the sputtering ions by the pressure

DOI:10.1088/1674-0068/20/06/706-710

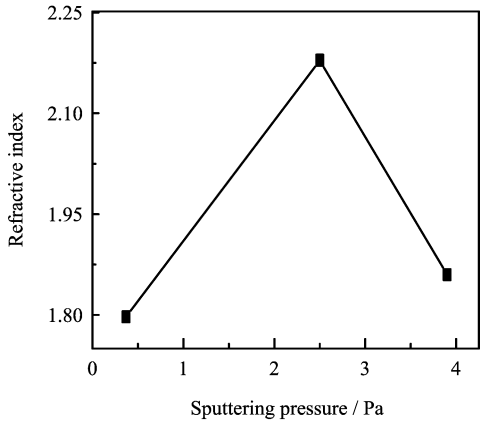

FIG. 5 The curve of refractive index of as-deposited thin films *vs.* pressure (at λ=550 nm).

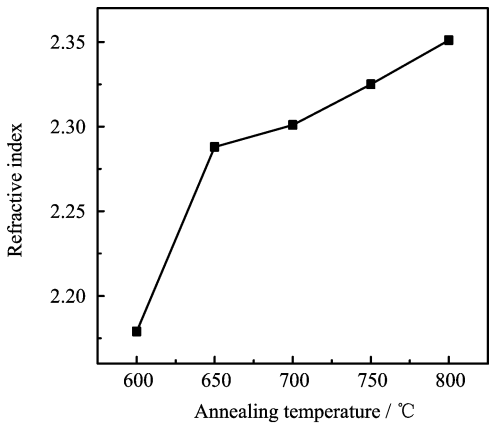

FIG. 6 Refractive index curve of $Ba_{0.65}Sr_{0.35}TiO_3$ thin films for as-deposited and post-deposited annealed at 650, 700, 750, and 800 °C (at λ=550 nm).

during the sputtering.

We assume that the Ar gas atoms after entering the chamber are ionized. At low sputtering pressure, the number of the sputtering ions (Ba^{2+}, Sr^{2+}, or Ti^{4+}) is few and the mean free path of sputtering ions is long. The sputtering ions with high kinetic energy would bring about resputtering. This reduces the films are provided with porosity. Hence, there is excessive scattering of the light in the wavelength region.

During the deposition, the sputtering ions that collide with Ar ions are scattered out of the flight path of the plume between target and substrate. When the sputtering pressure increases, we should take into account of the scattering of the sputtering ions. With the sputtering pressure increasing, the number of the sputtering ions obvious ascends. At the same time, the scattering of the sputtering ions is not strong. Therefore, the deposition rate reaches the maximum on the base of both two factors. The high deposition rate results in the films become compact and the grain size becomes larger [27]. Then the scattering of the light falls into a decline in the wavelength region, the refractive index of BST thin films increases.

When the sputtering pressure continues to increase, the scattering of the sputtering ions evidently becomes strong. The number and the kinetic energy of the sputtering ions that can reach the substrate rapidly descend. In this case, the films are full of defects, such as pores, impurities, and oxygen deficiency. Therefore, there is a relatively small reduction of the refractive index.

The ratio of oxygen to argon also has an important effect on properties of BST thin films prepared by RF magnetron sputtering. The oxygen to argon ratio affects the refractive index of as-deposited BST films. The refractive index has been found to increase from 1.998 to 1.860 with the ratio of oxygen to argon. This behavior may result from the change of the film stoichiometry, structure and texture, which are effected by the oxygen to argon ratio on two points. On one hand, the atomic mass of Ba is heavier than that of Sr, therefore the Ba atomic sputtering rate is relatively decreased when the ratio of oxygen to argon increases, and a high temperature deposition of BST film under non-oxidizing atmosphere, such as Ar, generally produces oxygen vacancies in the film [28]. On the other hand, the sputtered atoms collision increases which was caused by the increase of oxygen atoms and the mean free path being shorter. As a result, the film stoichiometry, structure and texture have been improved as the ratio of oxygen to argon increases. Thus, the refractive index of the films increases.

The refractive index of BST films is strongly dependent on the processing techniques. BST thin films have been deposited at 600 °C with the sputtering pressure of 2.5 Pa and the oxygen to argon ratio of 1:4. In succession, the as-deposited films anneal at 650, 700, 750, or 800 °C. As shown in Fig.6, the refractive index increases with annealing temperature increasing. The increase of refractive index can be attributed to the sputtering process that produces films with porous microstructure and consequently a packing density is lower than unity. However, as the annealing temperature increases, both mass and packing density of the films increase, resulting in an increase in the refractive index. The relationship between the packing density and refractive index of films has been discussed in detail by earlier works and it has been found that when the film achieves the buck value of index its packing density is the highest [29]. Thus, it is reasonable to assume that one of the causes for increase in refractive index with temperature for the films in the present case is the increase in their packing density.

IV. CONCLUSION

Thin films of $Ba_{0.65}Sr_{0.35}TiO_3$ (BST) have been prepared on the fused quartz substrates with radio frequency magnetron sputtering. XRD patterns shows

DOI:10.1088/1674-0068/20/06/706-710

BST thin films deposited at 600 °C and subsequently annealed at 700 °C have a perovskite phase with a pseudocubic structure, and the observed diffraction peaks are (100), (110), (111), (200), and (210) within the 2θ range from 20° to 67°, and the characteristic XRD peaks is sharp and more intense. The FESEM and AFM images indicated that the film was dense and finegrained and the surface of the film was smooth, crack-free and pore-free. The cross-sectional FESEM image revealed that the film integrated with the substrate closely and there was no obvious interdiffusion. The transparency of the thin films decreased and the absorption edge of the thin film shifted towards longer wavelengths with increasing postdeposition temperature. And the refractive index of BST thin films has also been studied. It is found that the substrate temperature, sputtering pressure, ratio of argon to oxygen and annealing temperature all affect the refractive index of BST thin films. There is a 10% variation of refractive index for BST films deposited over a substrate temperature range of 560 °C to 650 °C without annealing. This could be due to the mobility and the total energy at different substrate temperature. In the range of the sputtering pressure from 0.37 Pa to 2.5 Pa, the refractive index of as-deposited BST thin films increases with the pressure. However, when the pressure increases up to 3.9 Pa, the refractive index reduces to 1.860. The behavior of the refractive index results from the number and the kinetic energy of the sputtering ions. The refractive index has been found to increase with the ratio of oxygen to argon. The main reason is the improvement of the film stoichiometry and texture, which are affected by the ratio of oxygen to argon. The refractive index increases with annealing temperature is due to the increase of the packing density of the films. Finally, the refractive index of BST thin films is essentially affected by the films microstructure and texture.

V. ACKNOWLEDGMENTS

This work was supported by the National Natural Science Foundation of China (No.50672022), the Natural Science Foundation of Hubei Province (No.2004ABA094), and the Innovation Team Foundation of Education Bureau of Hubei Province, China.

[1] H. Zhu, J. M. Miao, and M. Noda, Sensors and Actuators A **110**, 371 (2004).
[2] S. J. Liu, X. B. Zeng, and J. H. Chu, Microelecreonics J. **35**, 601 (2004).
[3] C. B. Samantaray, A. Dhar, and D. Bhattacharya, J. Mater. Sci. Mater. El. **12**, 365 (2001).
[4] J. Li, F. Duewaer and C. Gao, Appl. Phys. Lett. **76**, 769 (2000).
[5] D. C. Yoo and J. Y. Lee, J. Cryst. Growth **224**, 251 (2001).
[6] Jaemo Im, O. Auciello, P. K. Baumann, S. K. Streiffer, D. Y. Kaufman, and A. R. Krauss, Appl. Phys. Lett. **76**, 625 (2000).
[7] C. C. Hwang, M. H. Juang, M. J. Lai, C. C. Jaing, J. S. Chen, S. Huang, and H. C. Cheng, Solid-State Electronics **45**, 121 (2001).
[8] E. J. Cukauskas, S. W. Kirchoefer, and W. Chang, J. Cryst. Growth **236**, 239 (2002).
[9] C. L. Huang and Y. C. Chen, Mater. Sci. Eng. A **345**, 106 (2003).
[10] R. Thielsch, K. Kaemmer, and B. Holzapfel, Thin Solid Films **301**, 203 (1997).
[11] B. Panda, A. Dhar, and G. D. Nigan, Thin Solid Films **332**, 46 (1998).
[12] H. Y. Tian, W. G. Luo, and X. H. Pu, J. Phys: Condens. Mater. **13**, 4065 (2001).
[13] F. M. Pontes, E. R. Leite, and D. S. L. Pontes, J. Appl. Phys. **91**, 5972 (2002).
[14] P. Petrik, N. Q. Khanh, and Z. E. Horvath, J. Non-Cryst. Solids **303**, 179 (2002).
[15] S. C. Roy, G. L. Sharma, and M. C. Bhatnagar, Appl. Surf. Sci. **236**, 306 (2004).
[16] Z. M. Xu, Y. C. Tanushi, and M. Suzuki, Thin Solid Films **515**, 2326 (2006).
[17] S. J. Lee, K. Y. Kang, S. K. Kan, and M. T. Lanagan, Integrated Ferroelectrics **24**, 33 (1999).
[18] X. Tang, Ferroelectrics **232**, 83 (1999).
[19] J. P. Valleau, R. Ivkov, and G. M. Torrie, J. Chem. Phys. **95**, 523 (1991).
[20] H. Y. Tian, J. Choi, K. No, and K. T. Kim, Mater. Chem. Phys. **78**, 138 (2003).
[21] J. C. Manifacier, J. Gasiot, and J. P. Fillard, J. Phys. E **9**, 1002 (1976).
[22] F. K. Shan and Y. S. Yu, J. Eur. Ceram. Soc. **24**, 1869 (2004).
[23] G. Xu, P. Jin, and M. Tazawa, Thin Solid Films **425**, 196 (2003).
[24] D. Y. Wang, C. L. Mak, K. H. Wong, H. L. W. Chan, and C. L. Choy, Ceram. Int. **30**, 1745 (2004).
[25] T. J. Zhang, S. Z. Li, B. S. Zhang, W. H. Huang, and R. K. Pan, Key. Eng. Mater. **336**, 79 (2007).
[26] S. C. Seel and C. V. Thompson, J. Appl. Phys. **88**, 7079 (2000).
[27] Z. B. Fang, Z. J. Yan, and Y. S. Tan, Appl. Surf. Sci. **241**, 303 (2005).
[28] T. J. Zhang, S. Z. Li, B. S. Zhang, R. K. Pan, J. Jiang, and W. H. Huang, Jpn. J. Appl. Phys. **44**, 8599 (2005).
[29] K. Goedicke, J. S. Liebig, and O. Zywitzki, Thin Solid Films **377**, 37 (2000).

DOI:10.1088/1674-0068/20/06/706-710